DOSE DISTRIBUTION FUNCTIONS FOR NEUTRONS AND GAMMA-RAYS IN ANTHROPOMORPHOUS AND RADIOBIOLOGICAL PHANTOMS*

T. D. JONES, J. A. AUXIER, J. W. POSTON and D. R. JOHNSON
Health Physics Division,
Oak Ridge National Laboratory,
Oak Ridge, Tennessee

Abstract—A right circular cylinder, 30 cm in diameter and 60 cm in height, was assumed to be composed of standard soft tissue, and dose as a function of penetration depth was computed for plane beams of incident neutrons. Data are presented for monoenergetic neutrons of various energies up to 14.0 MeV as well as for the neutron spectrum from the Health Physics Research Reactor (HPRR). The calculations were of a Monte Carlo nature using a slightly revised version of Snyder's linear energy transfer (LET) code.[1] New LET curves were obtained for C, N, O, B, Be, protons, tritons, and alpha particles, and recently obtained values of cross sections for these same elements were used with the code.[2] Many previous theoretical treatments of similar problems tended to ignore inelastic scattering reactions due to (1) the complexity of coding, (2) the difficulty of obtaining appropriate inelastic cross sections, and (3) inadequate "fast memory" capacity of many computational machines. Results of these calculations were compared with (1) those for the infinite slab 30 cm thick in the National Bureau of Standards (NBS) Handbook 63, (2) those obtained for a burro cadaver exposed to the neutron spectrum from the HPRR,[3] and (3) those presented by Auxier *et al.*,[4] in their description of a belt containing various radiation detection devices to be used in the determination of the orientation of persons exposed to unscheduled criticality excursions.

THE Monte Carlo Linear Energy Transfer (LET) code used by Snyder in previous work [1, 5] has been modified and extended so that a more realistic treatment of various exposure situations is now possible. New stopping-power data[6] have been obtained for ions of C, N, O, B, Be, protons, tritons, and alpha particles, and are shown in Fig. 1. These curves are similar to those previously used by Snyder[1] for ions of C, N, O, and protons, except the low energy tail is now assumed to fall as the inverse power of velocity rather than the inverse power of energy. The code has been extended to include neutron inelastic scattering reactions in which the emitted neutron is assumed to come off isotropically in the center of mass system. For elastic scattering, preliminary calculations were made for incident neutron energies of 7 and 14 MeV. An energy cutoff of 2.5 MeV was used to determine the maximum influence of the assumption that all reactions were of an isotropic nature. The phantom is shown at the bottom of Table 1, and the results of the calculations are as shown in the table. Although the errors due to the assumption of isotropy are well within the bounds of the values of the coefficients of variation given in columns 4 and 6, the calculations, for the elastic case, were made without this simplifying assumption. Cross-sections used in the code were presented by Auxier (a complete discussion of the 33 nuclear cross-sections would be much too extensive for this paper) in his paper entitled "Neutron Cross-Sections and Reaction Products for H, C, N, and O for the Energy Range from Thermal to 15 MeV", and calculations were made for various

* Research sponsored by the U.S. Atomic Energy Commission under contract with the Union Carbide Corporation.

Table 1. Results of an Isotropic Treatment of Anisotropic Reactions in a Slab Phantom

Energy (MeV)	Slab no.	Isotropic $\left(\frac{\times 10^{-8}\ \text{rad}}{\text{neutron cm}^2}\right)$	C. of V. (%)	Anisotropic $\left(\frac{\times 10^{-8}\ \text{rad}}{\text{neutron cm}^2}\right)$	C. of V. (%)	Error (1-iso./aniso.) × 100 (%)
7 (2.5 cutoff)	1	0.456	6.8	0.448	6.2	− 1.8
	2	0.253	7.1	0.249	10.4	− 1.7
	3	0.120	10.8	0.126	15.9	+ 4.8
	4	0.054	12.0	0.059	17.0	+ 9.5
14 (2.5 cutoff)	1	0.526	7.2	0.457	6.4	−11.5
	2	0.336	8.3	0.323	9.9	− 4.1
	3	0.192	11.5	0.196	10.2	+ 2.3
	4	0.099	17.4	0.115	11.3	+14.2
14 (no energy cutoff)	1	0.562	6.2	0.484	6.2	−16.1
	2	0.329	11.5	0.332	7.2	+ 0.8
	3	0.203	9.8	0.214	8.9	+ 5.2
	4	0.106	11.3	0.137	19.7	+22.6

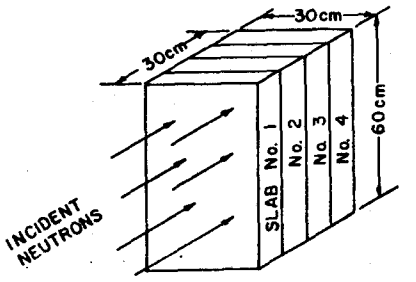

SLAB PHANTOM

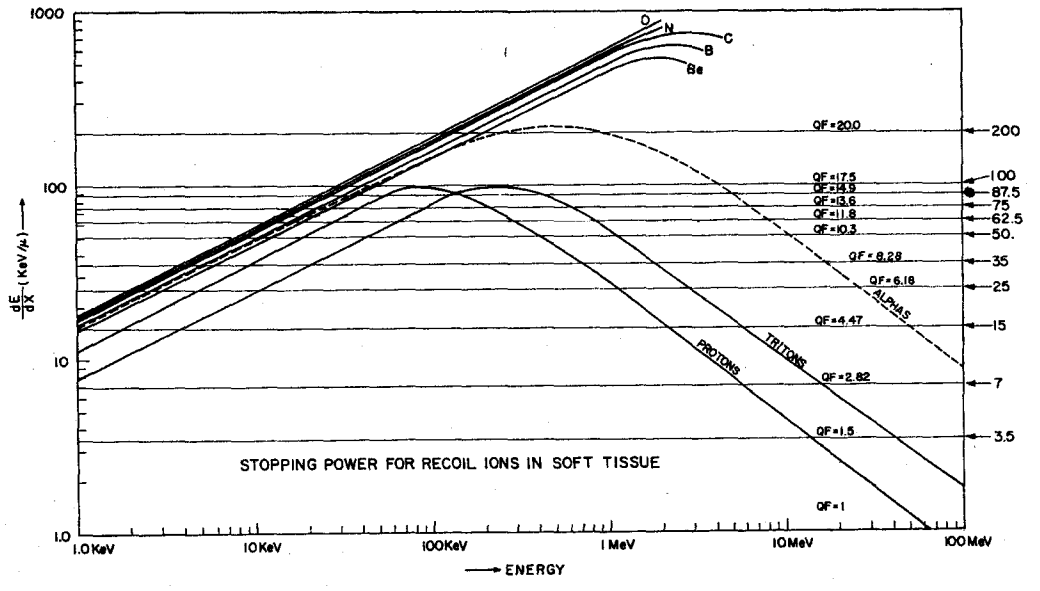

FIG. 1. Stopping power for recoil ions in soft tissue.

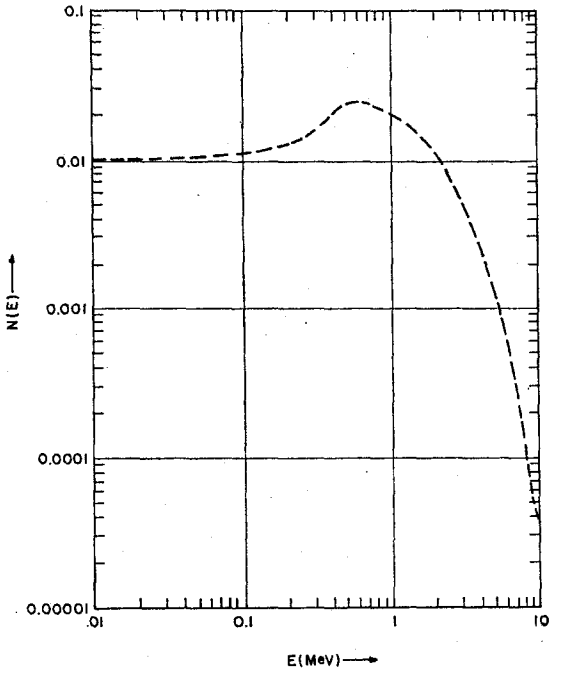

FIG. 2. Neutron leakage spectrum from HPRR.

monoenergetic neutron beams as well as the Health Physics Research Reactor (HPRR) neutron spectrum.[7, 8] The HPRR is an unshielded critical assembly of enriched ^{235}U[9] producing neutrons having the spectral distribution shown in Fig. 2. The exposure situation was assumed to be a plane parallel beam of neutrons incident unilaterally on the cylindrical phantom shown in Fig. 3. The cylinder was assumed to be 15 cm in radius and 60 cm high, composed of H,

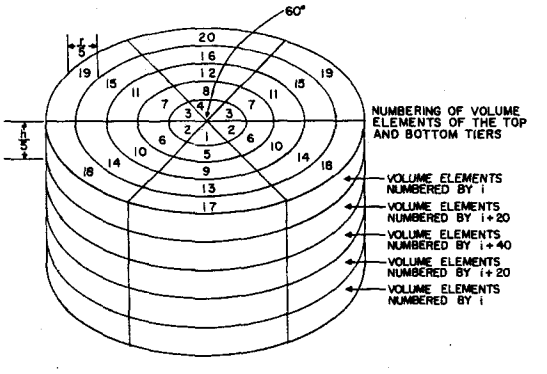

FIG. 3. Numbering of volume elements in the cylindrical phantom.

C, N, and O in the proportions found in standard, soft tissue.[10] The cylinder was subdivided into 150 volume elements, but due to geometrical symmetry, only 60 different elemental exposures were possible.

Table 2 shows the list of reactions that may occur in the phantom and the contribution averaged over the entire phantom from each of the various reactions. From this it is evident that many of the 33 possible reactions could have been ignored since they contribute an almost insignificant amount to the total dose. The reactions are listed in three groups. The reactions in the first group, numbers 1 through 4, are those of elastic scattering of neutrons by the nuclei in the medium. The second group, numbers 5 through 16, is that of the inelastic type in which a nucleus absorbs a neutron and is raised to an excited state and emits a neutron or two, in the case of the C(n, $2n'$) reaction, and one or more gamma-rays. The third group is that of the absorption type, in which a neutron is captured by a nucleus and one or more charged particles are emitted with or without accompanying gamma-rays.

The absorbed dose as a function of penetration depth, due to neutron reactions exclusive of the neutron-produced gamma dose, and the dose as a function of penetration depth, due to neutron-produced gamma-rays, for representative energies are shown in Fig. 4. For instance, the n and γ curves for a specific energy could be summed to obtain the total dose for a particular exposure situation.

Dose equivalent as a function of penetration depth is shown in Fig. 5 and was obtained through the use of ICRP-recommended quality factors[11] shown in the inset of this figure. The absorbed dose was separated into 12 LET intervals, and quality factors denoted by the arrows, representing the mean quality factor for that particular interval, were used to compute the dose-equivalent curves shown in this figure. The coefficients of variation for both the

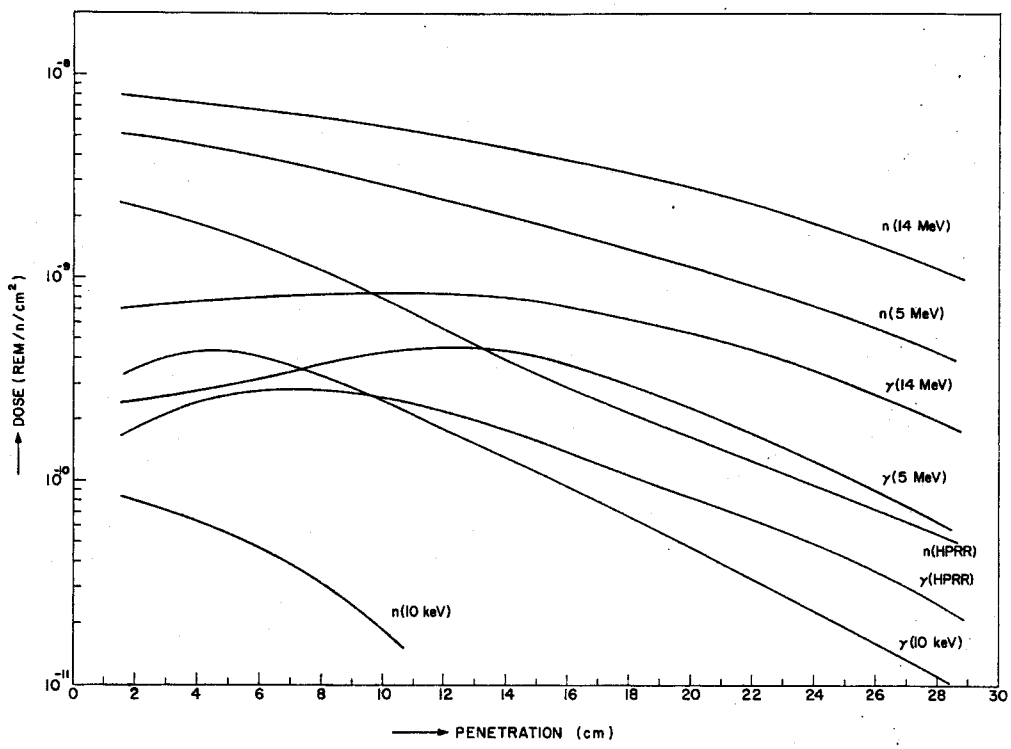

FIG. 4. Absorbed dose as a function of penetration depth in a cylindrical phantom (30 cm × 60 cm).

Table 2. Contributions to Dose Averaged over a Cylindrical Phantom from Reactions in Tissue

	Reaction	HPRR†	5 MeV†	7 MeV†	10 MeV†	14 MeV†
1.	H (n, n) H	6.9232	22.44	28.26	33.58	34.10
2.	C (n, n) C	0.1780	0.57	0.59	0.63	0.60
3.	N (n, n) N	0.0146	0.06	0.06	0.06	0.06
4.	O (n, n) O	0.4228	1.36	1.97	1.50	1.44
5.	C (n, n') *C; *C → C + γ_1; γ_1 = 1.75 MeV				0.05	0.03
6.	C (n, n') *C; *C → C + γ_2; γ_2 = 4.43 MeV	0.0099	0.03	0.26	0.59	0.69
7.	C (n, n') *C; *C → C + γ_3; γ_3 = 6.8 MeV	0.0001				0.14
8.	N (n, n') *N; *N → N + γ_1; γ_1 = 1.63 MeV	0.0004				0.01
9.	N (n, n') *N; *N → N + γ_2; γ_2 = 2.31 MeV	0.0002			0.02	0.03
10.	N (n, n') *N; *N → N + γ_3; γ_3 = 5.1 MeV	0.0001			0.03	0.02
11.	N (n, n') *N; *N → N + γ_4; γ_4 = 10.0 MeV					0.03
12.	N (n, n') *N; *N → N + γ_5; γ_5 = 11.0 MeV					0.03
13.	O (n, n') *O; *O → O + γ_1; γ_1 = 6.1 MeV	0.0083		0.14	1.36	1.54
14.	O (n, n') *O; *O → O + γ_2; γ_2 = 7.12 MeV	0.0036			0.30	0.38
15.	O (n, n') *O; *O → O + γ_3; γ_3 = 3.8 MeV					1.58
16.	O (n, n') *O; *O → O + γ_4; γ_4 = 4.8 MeV					0.77
17.	C (n, α_2) *Be; *Be → Be + n; Be → 2α					0.58
18.	C (n, n') *C; *C → Be + α					0.51
19.	N $(n, 2N)$ N					0.01
20.	H (n, γ) H	1.7250	1.64	1.41	1.21	0.89
21.	C (n, α_0) Be	0.0006			0.11	0.36
22.	N (n, α_0) B	0.0127	0.10	0.06	0.10	0.11
23.	O (n, α_0) C	0.0284	0.55	0.69	0.73	1.11
24.	C (n, α_1) *Be; *Be → Be + γ; γ = 1.75 MeV	0.0001				0.05
25.	N (n, α_1) *B; *B → B + γ_1; γ_1 = 2.1 MeV	0.0006	0.01	0.01	0.02	0.04
26.	N (n, α_2) *B; *B → B + γ_2; γ_2 = 4.5 MeV	0.0001		0.01	0.02	0.05
27.	N (n, α_3) *B; *B → B + γ_3; γ_3 = 5.0 MeV	0.0004			0.04	0.06
28.	O (n, α_1) *C; *C → C + γ_1; γ_1 = 3.1 MeV	0.0014			0.11	1.03
29.	O (n, α_2) *C; *C → C + γ_2; γ_2 = 3.8 MeV	0.0009			0.22	2.46
30.	O (n, α_3) *C; *C → C + γ_3; γ_3 = 7.0 MeV					1.00
31.	N (n, p) *C	0.1495	0.19	0.22	0.22	0.18
32.	O (n, p) *N; *N → N + γ; γ = 6.1 MeV					0.51
33.	N (n, t) C			0.01	0.01	0.02
	Total doses	9.4809	26.95	33.69	40.91	50.42

† × 10^{-10} rad/neutron/cm^2.

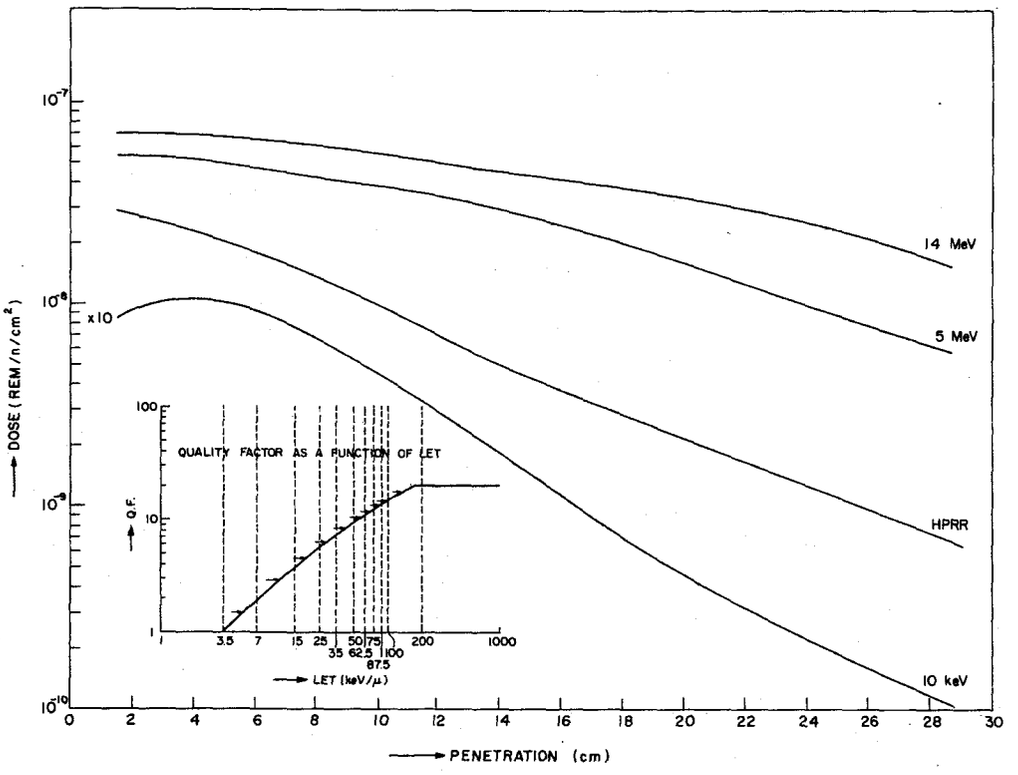

FIG. 5. Dose equivalent as a function of penetration depth in a cylindrical phantom (30 cm × 60 cm).

rad and rem dose curves range from about 7% at the front where the volume elements are large to 22% at the center where they were much smaller to about 17% at the rear where the volume elements are large, but the statistical parameters are influenced by the exponential nature of the attenuation of neutrons. For the spectrum from the HPRR, the coefficients of variation range from 5% at the front to 40% at the center and rear. The determinant factor here is the statistical nature of the energy of the incident neutrons.

Figure 6 shows dose as a function of LET for incident neutrons of energies 2.5, 5, and 14 MeV at penetration depths of 1.5, 13.5, and 28.5 cm. This illustrates the changing LET spectrum with both penetration depth and energy. For example, the LET spectral distribution of dose for 5 MeV neutrons at a penetration depth of 1.5 cm is not very unlike that for 14 MeV neutrons at a penetration depth

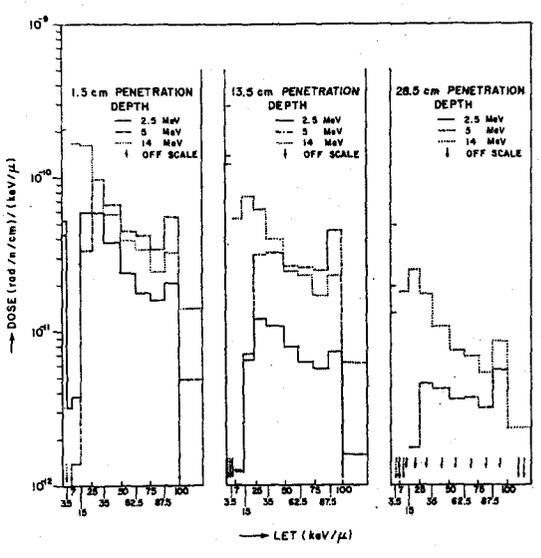

FIG. 6. Dose as a function of LET.

of 13.5 cm. Calculations of the above type have been completed for incident neutrons of representative energies between thermal and 14 MeV.

REFERENCES

1. W. S. SNYDER. The LET distribution of dose in some tissue cylinders, *Biological Effects of Neutron and Proton Irradiations*, Vol. 1, p. 3, IAEA, Vienna, 1964.
2. J. A. AUXIER and M. D. BROWN. Neutron cross-sections and reaction products for H, C, N, and O for the energy range from thermal to 15 MeV. This volume.
3. J. W. POSTON and D. R. JOHNSON. Oak Ridge National Laboratory. Personal communication, 1966.
4. J. A. AUXIER, F. W. SANDERS and P. N. HENSLEY. *Health Phys.* **5,** 226 (1961).
5. W. S. SNYDER. Distribution of dose and dose equivalent resulting from broad-beam irradiation of a man-sized cylindrical phantom by monoenergetic neutrons. Health Physics Society Meeting, Los Angeles, 1964.
6. D. R. DAVY. Oak Ridge National Laboratory. Personal communication, 1966.
7. Health Physics Division Annual Progress Report for Period Ending July 31, 1965. Oak Ridge National Laboratory Report ORNL-3849.
8. Health Physics Division Annual Progress Report for Period Ending July 31, 1964. Oak Ridge National Laboratory Report ORNL-3697.
9. J. A. AUXIER. *Health Phys.* **11,** 89–93 (1965).
10. Measurement of absorbed dose of neutrons, and of mixtures of neutrons and gamma rays. *Nat. Bur. Stand. Handbook* **75** (1961).
11. *Recommendations of the International Commission on Radiological Protection*, ICRP Publication 4, Report of Committee IV (1953–1959), Pergamon Press, 1964.